Free-Radical Polymerizations Associated with the Trommsdorff Effect Under Semibatch Reactor Conditions. IV. On-Line Inferential-State Estimation

G. B. BHARGAVA RAM, SANTOSH K. GUPTA, D. N. SARAF

Department of Chemical Engineering, Indian Institute of Technology, Kanpur - 208016, India

Received 30 August 1996; accepted 19 November 1996

ABSTRACT: A moving-horizon inferential-state estimation technique is described which uses simulated "experimental" data on temperature and viscosity to study *bulk* polymerization of free-radical systems. The short-term predictive capability of this technique is found to be quite good. A considerable amount of ringing (oscillations between the lower and upper bounds) is observed in the values of the estimated parameters which can be reduced significantly by narrowing down the range of parameter values or by including longer horizons in parameter estimation. Short-range prediction of viscosity was also found to be good. The model-calculated values of monomer conversion and molecular weights were found to be quite satisfactory in the entire range of operation. The long-term predictions of the model using the estimated parameters may or may not be accurate depending on the length of historical data used in the prediction. However, periodic use of state-variable estimation based on all the data up to that time, followed by the determination of the optimal temperature history in the future, could be a feasible strategy for experimental on-line optimizing control of bulk free-radical polymerizations which exhibit significant amounts of the Trommsdorff effect.
 J Appl Polym Sci **64:** 1861–1877, 1997

INTRODUCTION

In free-radical polymerizations, the termination, propagation, and initiation reactions (see Table I) become diffusion-controlled as the conversion of the monomer increases and the viscosity of the reaction mass increases. The manifestations of these diffusion-controlled reactions (sharp and large increases in monomer conversion, x_m, with time after a certain period, increase in the weight-average chain length, μ_w; see Nomenclature for symbols and definitions) are commonly referred to as the gel (or Trommsdorff),[1,2] glass, and cage effects, respectively. A good model is required to account for these effects mathematically, so that it can be used for design, optimization, and control purposes. A sample polymerization system exhibiting these phenomena is that of polymethyl methacrylate (PMMA), an important commodity plastic.

A vast amount of research has been reported in the open literature in the last two decades on the development of theoretical models for MMA polymerization. Chiu et al.[3] developed a model having a molecular basis and used the Fujita–Doolittle free-volume theory to account for the diffusional limitations of the termination and propagation rate constants, k_t and k_p. In this model, a set of algebraic equations were written for the gel and glass effects, using the initial number-average chain length, $\mu_{n,0}$, as a parameter. Later, Achilias and Kiparissides[4,5] developed a model using the free-volume theory of Vrentas and Duda[6] and accounted for the diffusional effects on k_t and k_p, as well as the initiator efficiency, f. This model used the initial concentration of the initiator, $[I]_0$,

Correspondence to: D. N. Saraf.
 CCC 0021-8995/97/101861-17

as a parameter. Normally, industrial reactors are operated under nonisothermal or semibatch conditions with addition and removal of components like initiator, solvent, and monomer. The models of Chiu et al. and Achilias and Kiparissides cannot be applied to these situations since the value of $\mu_{n,0}$ or $[I]_0$ is not precisely defined for such cases. Ray et al.[7] developed a model which did not have such limitations. They assumed the initiator efficiency to be constant and obtained expressions for two parameters of the model, $\theta_t(T)$ and $\theta_p(T)$, by curve-fitting experimental data[8,9] taken in small ampules under isothermal conditions. The predictions made by their model for idealized, nonisothermal conditions (step changes in temperature) as well as for idealized semibatch operating conditions (intermediate addition of a solution of initiator in monomer) were found to be in good agreement with experimental observations.[10,11] This confirmed the adequacy of the model for the simulation of polymerizations under industrially relevant conditions of operation.

More recently, Seth and Gupta[12] modified the model of Ray et al.[7] and also considered the variation of the initiator efficiency, f, with time. Their model used three parameters, $\theta_t(T)$, $\theta_p(T)$, and $\theta_f(T)$, representing the gel, glass, and cage effects, respectively. They again curve-fitted the experimental data[8,9] on MMA polymerization under isothermal conditions in small ampules (both for bulk polymerization with an AIBN initiator[8] as well as for solution polymerization in benzene with benzoyl peroxide[9]). Predictions of their "tuned" model were found to be in better agreement with experimental data[10,11] taken under idealized nonisothermal and semibatch conditions than was the model of Ray et al. The complete set of equations for this model[12] and the values of several parameters and physical properties required are given in Appendices A and B.

With an appropriate model available for free-radical polymerizations, one can now think of studying the *on-line* optimizing control of these processes. An important step in such studies is the measurement of the *state* of the system at different times, t. Densitometers and gel permeation chromatography were used in some experimental control studies[13–15] of *solution* polymerizations for estimating monomer conversions, $x_m(t)$, and the number-average chain lengths, $\mu_n(t)$ [or the weight-average chain lengths, $\mu_w(t)$]. However, these experimental techniques cannot be used conveniently for *bulk* polymerizations, and inferential-state estimation techniques have to be resorted to. Seth and Gupta[12] and Chakravarthy et al.[16] suggested the use of experimental values of the viscosity, $\eta(t)$, of the reaction mass [along with the measured values of the temperature, $T(t)$] for such purposes. Recently, Embirucu et al.[17] surveyed the open literature on advanced control strategies for polymerization reactors and found that very few studies have been reported on property estimation techniques for the control of *bulk* polymerizations. There is, thus, a definite need to explore whether model-based inferential-state estimation using $T(t)$ and $\eta(t)$ is, indeed, feasible. If so, it could be used experimentally (in the future) for on-line optimizing control of bulk polymerization reactors. This study presents some theoretical work along these lines for the sample system, PMMA.

Table I Kinetic Scheme for Polymerization of MMA (Bulk and Solution Polymerizations)

1. Initiation	$I \xrightarrow{k_d} 2R$
2. Propagation	$R + M \xrightarrow{k_i} P_1$
3. Termination	$P_n + M \xrightarrow{k_p} P_{n+1}$
By combination	$P_n + P_m \xrightarrow{k_{tc}} D_{n+m}$
By disproportionation	$P_n + P_m \xrightarrow{k_{td}} D_n + D_m$
4. Chain transfer to monomer	$P_n + M \xrightarrow{k_f} P_1 + D_n$
5. Chain transfer to monomer via solvent	$P_n + S \xrightarrow{k_s} S^{\bullet} + D_n$
	$S^{\bullet} + M \xrightarrow{k_s} S^{\bullet} + D_n$
	or
	$P_n + M \xrightarrow{k_s} D_n + P_1$

FORMULATION

Model

The kinetic scheme for MMA polymerization is shown in Table I. A set of ordinary differential equations (ODEs) representing the mass balances and moment equations for a semibatch reactor can easily be written. These are of the form

$$d\mathbf{x}/dt = \mathbf{F}(\mathbf{x}); \quad \mathbf{x}(t = 0) = \mathbf{x}_0 \qquad (1)$$

where $\mathbf{x}(t)$ is the state variable vector defined by

$$\mathbf{x} = [I, M, R, S, \lambda_0, \lambda_1, \lambda_2, \mu_0, \mu_1, \mu_2, \zeta_m, \zeta_{m1}] \quad (2)$$

The kth ($k = 0, 1, 2$) moment of the radical and dead macromolecular species, P_n and D_n, respectively, are represented by λ_k and μ_k (see Nomenclature). The exact equations are shown in Appendix A. Equations (A.1)–(A.12) of this appendix account for intermediate additions and removals of components like initiator, solvent, and monomer through the terms R_{li}, R_{ls}, R_{lm}, R_{vs}, and R_{vm}. The conversion of monomer is defined as

$$x_m = 1 - (M/\zeta_{m1}) \quad (3)$$

where ζ_{m1} is the net monomer added to the reactor since the beginning of the operation.

The variation of the rate constants, k_t ($\equiv k_{td}$ for PMMA, since $k_{tc} \cong 0$), k_p, as well as the initiator efficiency, f, are described by the algebraic eqs. (A.13)–(A.27) in Appendix A.[12] It is observed that k_t, k_p, and f depend on the current values of T, μ_n, λ_0, V_1, etc., and not on the initial conditions as in the models of Chiu et al.[3] and Achilias and Kiparissides.[4,5] This is why the model of Seth and Gupta[12] can be applied easily to nonisothermal and semibatch operations of reactors. The values of several properties and parameters required to integrate the equations in Appendix A are given in Appendix B (for *bulk* polymerization of MMA using the AIBN initiator). The three parameters, $\theta_t(T)$, $\theta_p(T)$, and $\theta_f(T)$, have been expressed[12] in terms of second-order polynomials in $1/T$ as shown in Appendix B. The equations in Appendix A can be integrated (for a given set of initial conditions[12]) using the NAG library program, D02EJF (which uses Gear's technique[18]), to obtain histories of monomer conversion and the number- and weight-average chain lengths. The value of the parameter, TOL, required in this code was 10^{-7} (the results were insensitive to decreases in the value of TOL). The values of the coefficients a_1–a_3, b_1–b_3, and c_1–c_3 in the model were obtained earlier[12] by curve-fitting experimental data under isothermal conditions on bulk[8] and solution[9] polymerization at several temperatures. In the present work, the parameters a_1–a_3, b_1–b_3, and c_1–c_3 were retuned using only the bulk polymerization data[8] since these were of interest. These parameters were found to be quite close to the values obtained by Seth and Gupta,[12] and the new values are given in Appendix B.

An equation relating the viscosity, η, of the reaction mass and the temperature, T, to the state of the system (monomer conversion, x_m, and weight-average molecular weight, M_w) is required so that model-based inferential-state estimation can be done. Moritz[19] suggested the use of the Lyons–Tobolsky[20] equation. This equation is a one-term adaptation of the more general series expression relating the specific viscosity, $(\eta/\eta_{\mathrm{sol}}) - 1$, to the product of the intrinsic viscosity, $[\eta]$, and the polymer concentration, C_{polym}. We modified the Lyons–Tobolsky equation slightly to incorporate a higher-order (quadratic) term as shown in Appendix A [eq. (A.28)]. This was done to obtain better predictions for some preliminary experimental data on nonreacting PMMA–MMA solutions at 50 and 70°C, taken on a Haake® Rotovisco RV20 viscometer in our laboratory.[21] Such an empirical modification also helped in suppressing the temperature variation of the parameter b in the adapted Lyons–Tobolsky equation. The parameter k_H in this equation, which is a function of temperature, was tuned using the (preliminary) viscosity data generated in our laboratory, and two coefficients, d_1 and d_2, relating k_H to T using a linear variation, were so obtained. The values of d_1 and d_2 are given in Appendix B. It must be emphasized that more experimental data on the viscosity of (nonreacting) PMMA–MMA solutions at several *additional* temperatures and concentrations must be taken before the values of d_1 and d_2 (given in Appendix B) can be used for experimental studies. However, since the main objective of the present study was to explore whether viscosity measurements can be successfully used for model-based, on-line inferential-state estimation, the use of the order-of-magnitude estimates of d_1 and d_2 given in Appendix B (based on the results taken over a restricted range of experimental conditions) is appropriate.

Generation of "Experimental" Data

To explore the idea of using measured values of $T(t)$ and $\eta(t)$ for inferential-state estimation of bulk PMMA reactors, one needs to have experimental viscosity data for a given $T(t)$ for a polymerizing system. Since this is not yet available, (pseudo) "experimental" data are generated using the model itself, and some random noise is superposed on the "smooth" model-predictions to simulate actual experimental data. One of the optimal temperature histories for bulk polymerization of MMA, as recently provided by Chakravarthy et

al.,[16] is selected (desired value of $\mu_n = 1800$ and of monomer conversion, $x_m = 0.94$, to be obtained in the minimum reaction time) for this work. This smooth temperature history, $T_{sm}(t)$, is curve-fitted using a 17th-order Chebyshev series (using the NAG library program, E02ADF) so that it can be provided as an input to the reactor-simulation program. A white noise is superposed on $T_{sm}(t)$, using a random number, $[R(t)]$, generator to give what can be considered as the "experimental" temperature history, $T_{exp}(t)$:

$$T_{exp}(t_i) = T_{sm}(t_i) + [4R(t_i) - 2] \qquad (4)$$

In eq. (4), $R(t)$ is a random number lying between 0 and 1, generated using the NAG subroutine G05CCF. The term, $4R(t_i) - 2$, is used so as to give the amplitude of the noise as 2°C. The "experimental" data *points* are generated using eq. (4) with $t_i = i(\Delta t)$, where Δt is taken as 0.5 min. The viscosity of the reaction mass for bulk polymerization of MMA has then been generated using the initial value of the initiator concentration, $[I]_0$, as 15.48 mol/m^3 and using $T_{exp}(t_i)$ [with linear interpolation used between consecutive points of $T_{exp}(t_i)$ in D02EJF]. It is observed that the model values of $\eta(t)$ so obtained are quite smooth and we must, therefore, add on a noise again so as to provide simulated "experimental" viscosity data. The following equation is used for this purpose:

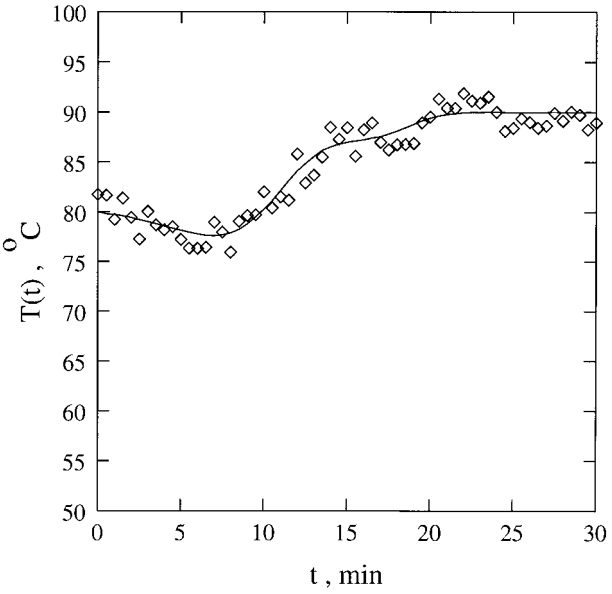

Figure 1 Continuous temperature history (solid curve) for $[I]_0 = 15.48$ mol/m^3 and randomized temperature "data" points used in this study.

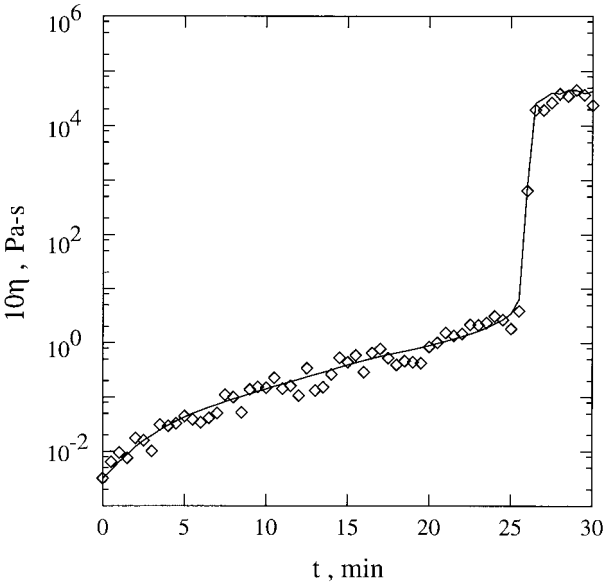

Figure 2 Viscosity (solid curve) of the reaction mass as generated using the temperature "data" points of Figure 1 with the model and best-fit values of the parameters as given in Appendix B. "Experimental" viscosity data (points) obtained on randomization also shown.

$$\eta_{exp}(t_i) = [0.5 + R(t_i)]\eta(t_i);\ t_i = i(\Delta t) \qquad (5)$$

Use of eq. (5) leads to fluctuations in η_{exp} ranging from 0.5η to 1.5η, a fairly large range as compared to the possible errors and fluctuations in real experimental viscosity data.

The "experimental" temperature and viscosity data so generated (by simulation) are shown in Figures 1 and 2. These data are used for studying model-based inferential-state estimation. The final values of x_m and μ_n using $T(t)$ given by the solid curve in Figure 1 are 0.9408 and 1748, respectively (these differ slightly from the values in Ref. 16 because our parameters are slightly different).

Inferential-state Estimation

In a typical polymerization reactor in which online optimizing control is implemented, one would have available, at time $t = t_1$, a set of experimental values of temperature and viscosity, $T_{exp}[i(\Delta t)]$ and $\eta_{exp}[i(\Delta t)]$; $i = 0, 1, 2, \ldots, t_1/(\Delta t)$. A short time-horizon for curve fitting, $t_1 - N_1(\Delta t) \le t \le t_1$, is selected and the experimental points lying (only) in this horizon are used to estimate the values of several of the parameters in the model. Sequential quadratic programming

Table II Initial Guesses and Bounds for Generating the Solution in the First Curve-fit Horizon and Parameters Used in the SQP Code

Parameter	Initial Guess	Lower Bound	Upper Bound
a_1	1.2416×10^2	1.2346×10^2	1.2446×10^2
b_1	8.0673×10^1	8.0071×10^1	8.1071×10^1
c_1	2.0168×10^2	2.014×10^2	2.024×10^2
d_1	0.3118	0.309×10^0	0.315×10^0
a_2	1.0314×10^5	1.03018×10^5	1.0334×10^5
b_2	7.5×10^4	7.4845×10^4	7.5168×10^4
c_2	1.445×10^5	1.4524×10^5	1.4556×10^5
d_2	9.93×10^{-4}	9.0×10^{-4}	1.0×10^{-3}
a_3	2.2735×10^7	2.2669×10^7	2.27743×10^7
b_3	1.765×10^7	2.75955×10^7	1.76999×10^7
c_3	2.7×10^7	2.6979×10^7	2.7083×10^7

Parameters in SQP Code[23]

Parameter	Value
tol_{ob}	10^{-3}
tol_{nl}	10^{-6}
func_{pr}	10^{-10}
tol_{act}	10^{-8}

(SQP)[22,23] was used in this work to obtain best-fit values of four parameters, a_1, b_1, c_1, and d_1 (referred to as a_1–d_1; while assuming all the remaining parameters to be the same as given in Appendix B—these being called *reference values* henceforth). The objective function used for the optimization is

$$\underset{a_1-d_1}{\text{Min}}\, E \equiv \sum_{i=t_1/(\Delta t)-N_1}^{t_1/(\Delta t)} \left[\frac{\eta_{\text{exp}}(t_i) - \eta_{\text{th}}(t_i)}{\eta_{\text{th}}(t_i)}\right]^2 \quad (6)$$

where η_{exp} is the experimental value of the viscosity, and η_{th}, the value predicted by the model corresponding to the values of a_1–d_1 used. To obtain the model values of the several state variables [see eq. (2)] and η_{th} for $t_1 - N_1(\Delta t) \le t \le t_1$ [as required in eq. (6)], the initial conditions are taken to be the *model* values at $t = t_1 - N_1(\Delta t)$ as computed in the previous iteration (and stored). Also, a constant temperature is assumed for the duration $t_1 - N_1(\Delta t) \le t \le t_1$, which is the average of the "experimental" values of temperature during this period. The NAG subroutine, E04UPF using SQP, was used for obtaining the best-fit values of a_1–d_1 [which minimize the sum of square error, E, in eq. (6)]. Table II gives the values of the computational parameters used with this code. The SQP procedure also requires initial guesses and bounds for the parameters a_1–d_1 for each value of t_1. The initial guesses supplied for the first iteration [$t_1 = N_1(\Delta t)$] are given in Table II. For subsequent values of t_1, the optimal values of the parameters in the previous iteration are used as the initial guess. The bounds on the parameters are also listed in Table II. The bounds on a_1–c_1 were chosen such that variations of about a decade (at any given temperature) are permitted in the values of θ_t, θ_p, and θ_f (note that a_1–c_1 are independent of temperature). The bounds on d_1 are chosen so as to permit a fairly large variation in the viscosity of the reaction mass. Much smaller bounds would normally be used in experimental on-line control work.

In addition to obtaining best-fit values of a_1–d_1 in any iteration of curve-fitting (parameter estimation mode), we used the same reactor simulation code to *predict* values of the state variables and of $\eta_{\text{th}}(t)$ for "future" times, $t_1 \le t \le t_1 + N_2(\Delta t)$ (prediction mode). These theoretical predictions could be compared with the "experimental" data points of viscosity (in the prediction horizon) to determine how good is the (short-term) predictive capability of the model-based state estimation technique described herein. A good model prediction capability is necessary if one wishes to use

model predictive control. The computer code starts from $t = 0$ and uses the first N_1 points (first curve-fitting horizon) for curve fitting (followed by prediction of N_2 points in the future). This completes the first iteration of curve fitting. The experimental values of viscosity for $0 + N_3(\Delta t) \leq t \leq (N_1 + N_3)(\Delta t)$ are then used for the second iteration (second curve-fitting horizon). This continues until the end of polymerization. The values of N_3 can be selected so as to have some overlap between the successive curve-fitting horizons.

A few checks were made on the computer code to ensure that it is free of errors. When the optimization program was run using *all* the "experimental" points (with no fluctuations introduced) and initial guesses were provided which differed from the reference values (Appendix B) of a_1–d_1, the optimization code converged to the reference values. Some other checks were also conducted and led to the conclusion that the code was reasonably free from errors. The CPU time taken for the optimization problem was about 30 s on a super-mini HP 9000/735 mainframe computer.

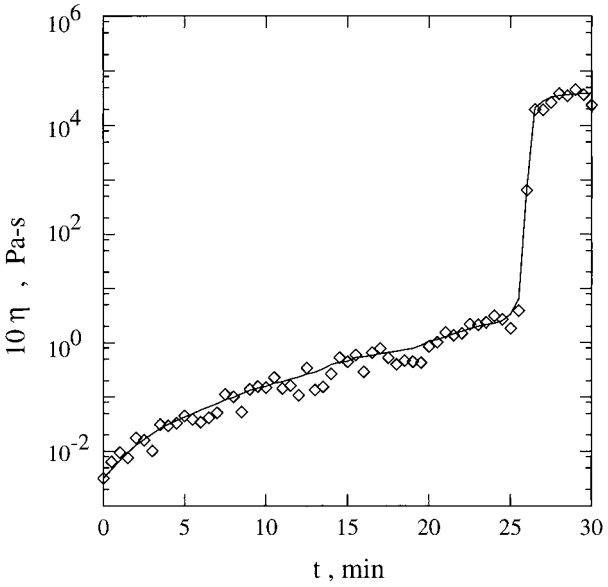

Figure 3 The curve-fitted viscosity (solid curve) for the reference case. "Experimental" viscosity data, shown by the points, are the same as in Figure 2.

RESULTS AND DISCUSSION

The optimization program was run on the "experimental" data of viscosity and temperature (Figs. 1 and 2), using the following parameters (called reference values again):

$$N_1 = 5$$
$$N_2 = 5$$
$$N_3 = 1$$
$$\Delta t = 0.5 \text{ min} \qquad (7)$$

Thus, five "data" points at a time are taken for curve fitting, and the curve-fitting horizon shifts by one "experimental" point at a time in this reference run (with four points common between consecutive curve-fitting horizons). The prediction horizon also consisted of five sampling intervals.

Figure 3 shows the piecewise fitted curve of $\eta(t)$ along with the "experimental" data points. The solid curve in Figure 3 consists of segments which extend for one Δt period (the nonoverlapping domain between two consecutive curve-fitting horizons). The fit of the viscosity "data" is seen to be quite good. Figure 4 shows the variations of the parameters a_1–d_1 from horizon to horizon (the end values of t of the curve-fitting horizons are shown in Fig. 4 on the abscissa). It is observed that there is a considerable amount of "ringing" in the values of these parameters between the lower and upper bounds. It is demonstrated *later* in this article that this is because we are trying to curve-fit only a small number (five) of experimental data points in any one parameter estimation and that the ringing can be reduced by lowering the bounds of the four parameters, as well as by increasing Δt. The corresponding variations in $\theta_t(T)$, $\theta_p(T)$, $\theta_f(T)$, and k_H are shown in Figure 5. The ringing in the values of a_1–d_1 are reflected as similar sharp fluctuations in the values of θ_t, θ_p, θ_f, and k_H. In addition, there is a general change in these parameters associated with their temperature dependence.[12] The monomer conversion, M_n and M_w, for the reference case are shown in Figures 6 and 7. It is observed that the model predictions agree quite well with the "experimental" points corresponding to the temperature "data" of Figure 1 (it may be noted that the viscosity "data" were generated by introducing additional fluctuations to values computed using the "data" of Figs. 6 and 7). The final values (at $t = 30$ min) of x_m and μ_n are found to be 0.9307 and 1743, respectively, for the curve-fitted case, as compared to the values of 0.9408 and 1748 corresponding to the temperature history shown by the solid (smooth) curve in Figure 1. The agreement is extremely good even though

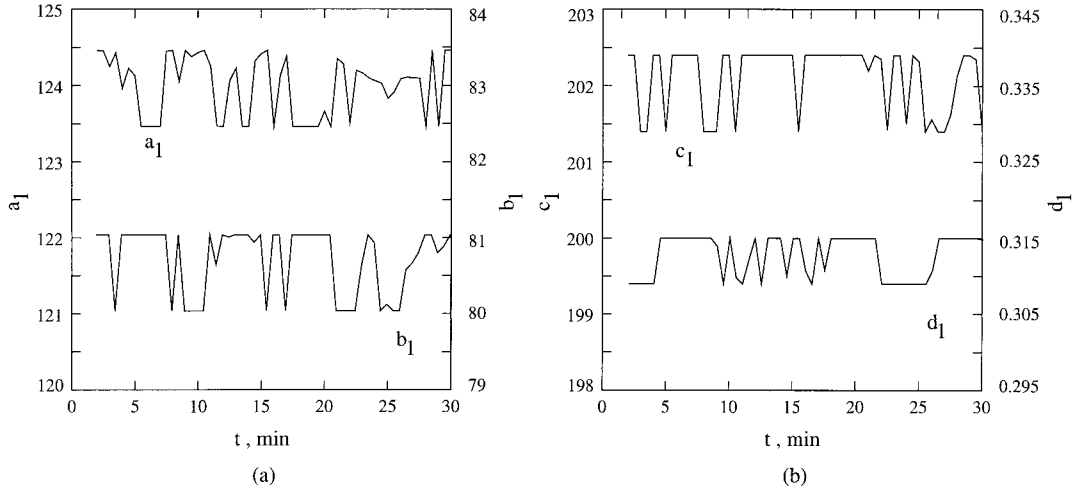

Figure 4 Variation of the parameters a_1–d_1 for the reference case, corresponding to the curve-fit of Figure 3.

temperature fluctuations of ±2°C and viscosity variations of ±50% were randomly introduced.

The optimal parameters obtained in any curve-fitting horizon are used with the temperatures in the corresponding prediction-horizon (five further points, since $N_2 = 5$) to predict the viscosity. The short-term prediction capabilities are shown in Figure 8. It is clear from this figure that if the curve-fitting horizon is far ahead of the gel effect, the short-term ($N_2 = 5$) predictions are quite good. When the curve-fitting horizon lies just before the gel effect, the short-term future predictions need not be excellent. The predictions, however, improve considerably when *even a single data point* from the gel-effect region is included in the curve-fitting horizon. This is shown in Figure 8(b). Similar results are obtained for short-term predictions of x_m, μ_n, and μ_w. All these reference results indicate that "experimental" data on $T(t)$ and $\eta(t)$ can, indeed, be used with a model to estimate the state variables of the system, e.g., $x_m(t)$, $\mu_n(t)$, and $\mu_w(t)$.

It may be added that long-term predictions using the present technique are also very good except when only a few (e.g., five) points are used in curve-fitting [see Figs. 9(a) and 10(a)]. However, use of another set of five points leads to better long-term predictions, as shown in Figures 9(b) and 10(b). This variation in the quality of the long-term prediction is a consequence of the

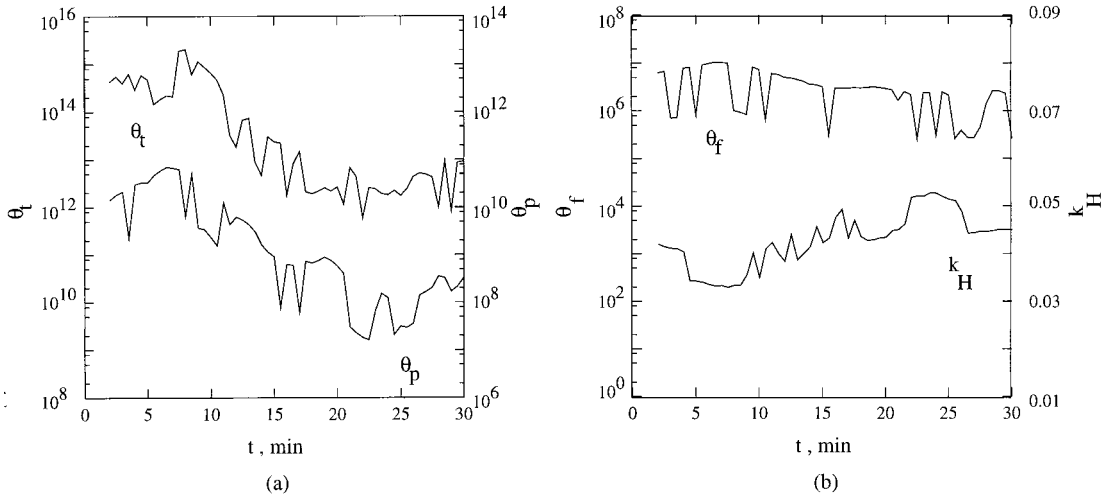

Figure 5 Variation of the parameters $\theta_t(T)$, $\theta_p(T)$, $\theta_f(T)$, and $k_H(T)$ corresponding to the curve-fit of Figure 3 (reference case).

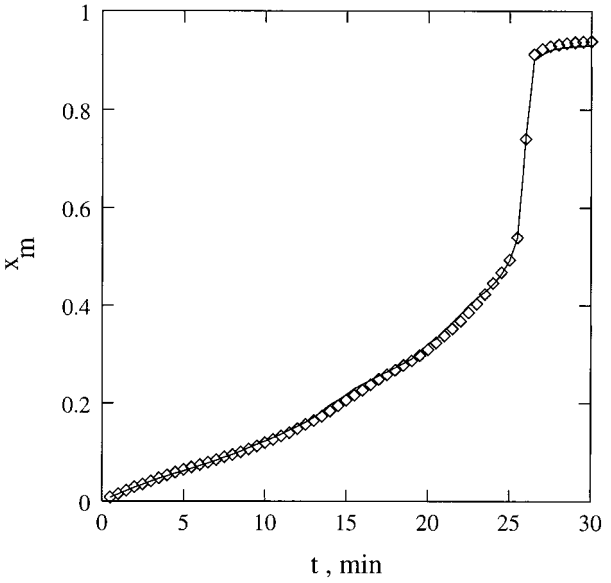

Figure 6 Estimated values of the monomer conversion (solid curve) for the reference case along with the "experimental" data.

ringing in the values of the parameters and does not arise when a larger curve-fitting horizon is used. For on-line optimizing control purposes with minimization of the reaction time as the objective function, we should use all the data up to time t_1, rather than five points, whenever fresh optimization is carried out.

Having established the applicability of the technique described herein for inferential state-variable estimation, we now study the effect of varying several of the other parameters involved. Instead of using the most recent optimal values of a_1–d_1 as the initial guess values for any curve-fitting horizon, we used the initial values given in Table II for *all* the horizons. There was no perceptible change in the fit of the $\eta(t)$ data. Almost the same degree of ringing of the parameter values was observed. The CPU time was also about the same (increased by about 1 s). These and other results not included in this article for reasons of brevity can be supplied on request.

In the reference run, we assumed a_2, a_3, b_2, b_3, c_2, c_3, and d_2 to be constants (at the values given in Table II), and we obtained best-fit values of a_1, b_1, c_1, and d_1. We explored if there would be any improvement if all the 11 parameters (a_1–d_2) were used for curve-fitting the $\eta(t)$ "data." The bounds of the remaining seven parameters provided to the SQP code, as well as the initial guesses, are also given in Table II. The bounds on a_2, a_3, b_2, b_3, and c_2, c_3 were selected so that each of them individually could give variations of about a decade in the values of θ_t, θ_p, and θ_f. The CPU time increased by about fourfold, to 111 s. We observed that there was not much improvement in the fit of the viscosity data. Also, the degree of ringing in the 11 parameters did not decrease much. Much larger oscillations were observed in the plots of $\theta_t(T)$, $\theta_p(T)$, and $\theta_f(T)$ for this case, possibly because of the adding-up of the effects of each of the additional parameters. Use of 11 parameters is, thus, not recommended since it provides no additional advantages over the use of four parameters (reference case).

We also studied the effect of narrowing the bounds on a_1–d_1 by about 50%. The final fit of the viscosity data was about as good as that observed for the reference run (Fig. 3). But the ringing of the parameters a_1–d_1 was reduced, as shown in Figure 11. Figure 12 shows the corresponding plots of θ_t, θ_p, θ_f, and k_H as functions of time. No worsening was observed in the short-term prediction capabilities. The final values of x_m, M_n, and M_w were observed to be close to the reference values. The CPU time decreased to 10 s. It can, thus, be inferred that narrowing the bounds for a_1–d_1 is desirable for experimental, on-line optimizing control. A comparison of Figure 12 with Figure 5 shows that by reducing the bounds the random fluctuations in the parameter values (which are indeed artifacts of the optimization procedure used) become significantly reduced but the sys-

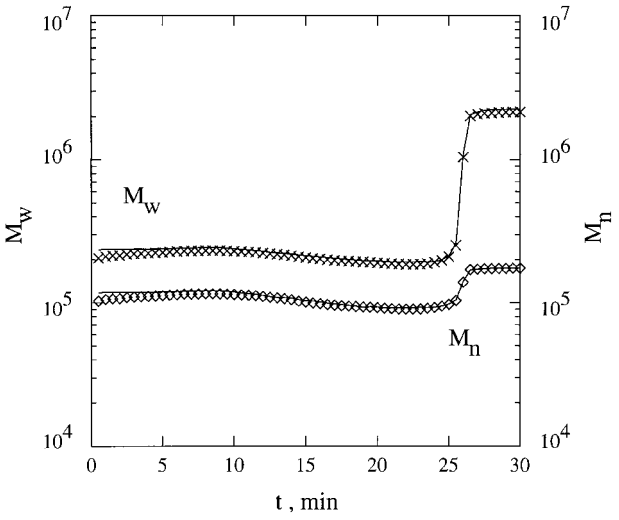

Figure 7 Estimated values of M_n and M_w (solid curve) for the reference case. "Experimental" data on M_n and M_w obtained using the temperature "data" of Figure 1 with the best-fit values of the parameters (Appendix B) in the model shown by the points.

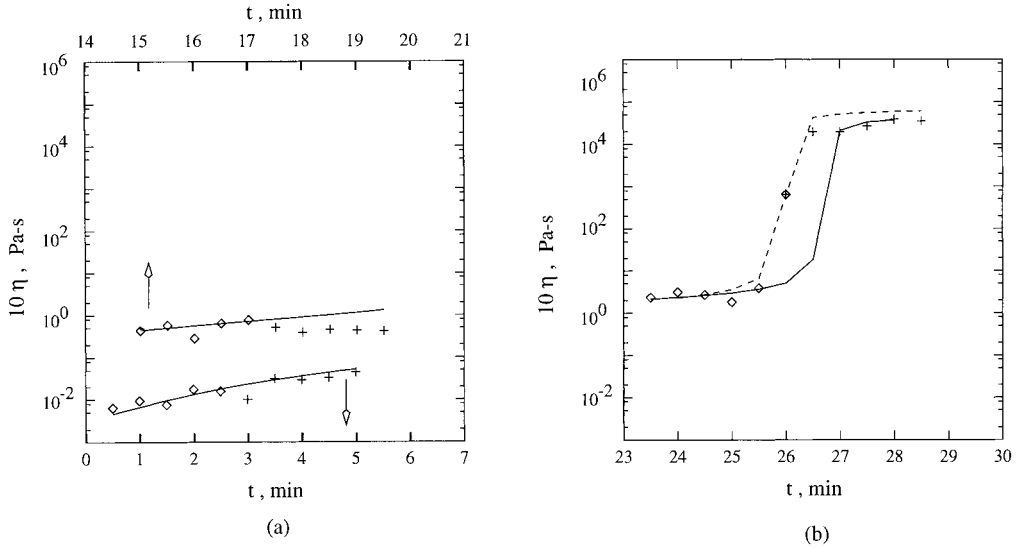

Figure 8 Short-range predictions for four curve-fitting horizons (reference case). Diamonds indicate the "data" on η used for curve-fitting, while pluses indicate the "data" in the prediction horizon. In (b), the solid curve uses the first five points (starting from t = 23.5 min) for curve fitting, while the dotted curve uses the five data points starting from t = 24 min.

tematic variations of these parameters, because of changes in temperature, are preserved. This justifies the reduction in the bounds. In all the cases studied, it was possible to estimate the state of the system (monomer conversion and average molecular weight) quite accurately and *uniquely* from the "experimental" viscosity and temperature data.

We next studied the effect of increasing the value of N_1, the number of points used in the curve-fitting horizon, from five to eight. The fit of viscosity was observed to be as good as that shown in Figure 3. The fluctuations in a_1–d_1 reduced slightly as compared to the reference case, as shown in Figure 13. The final values of x_m, M_n, and M_w were in the desired range, as in the reference case. The prediction capabilities were also found to be about the same as for the reference case. The CPU time came down, as expected, to 15 s.

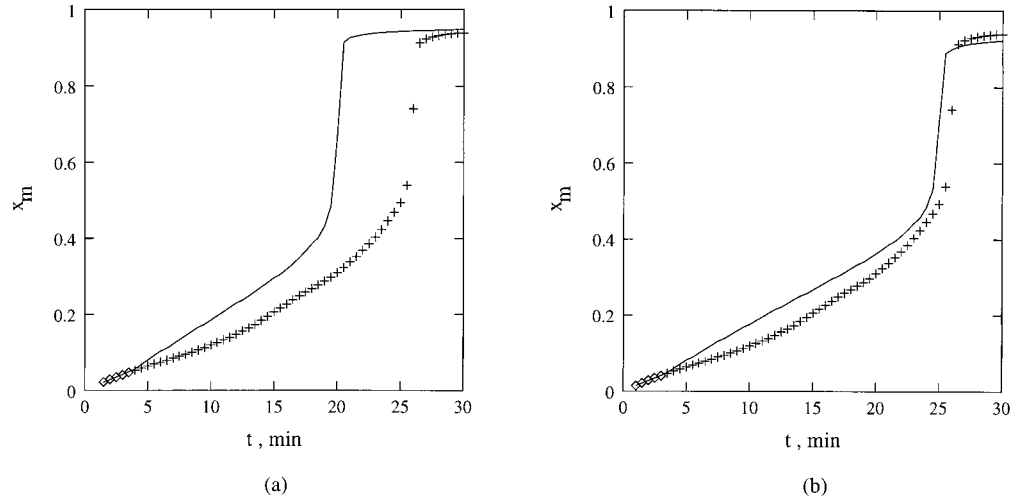

Figure 9 Long-range predictions for x_m (reference case) for two curve-fitting horizons. Notation same as in Figure 8.

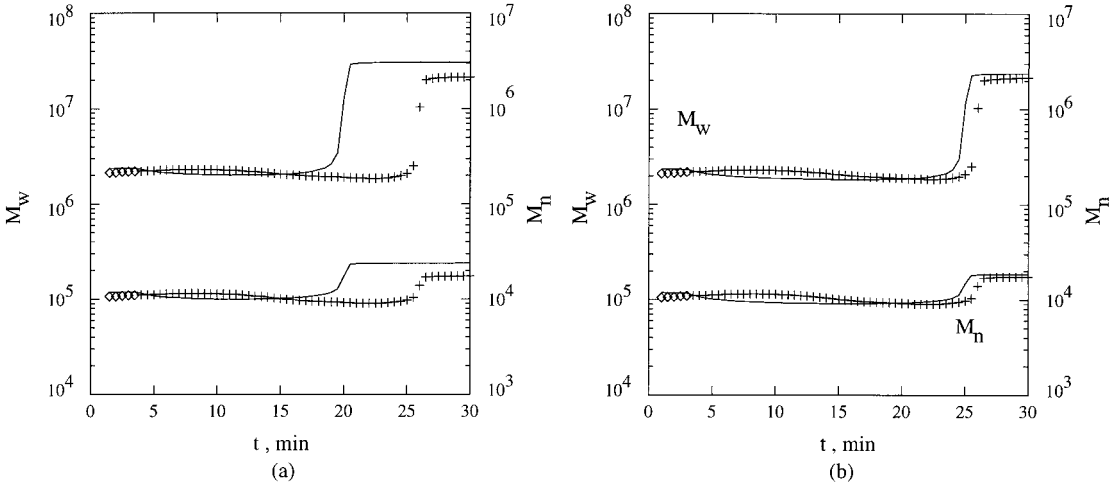

Figure 10 Long-range predictions for M_n and M_w (reference case) for two curve-fitting horizons. Notation same as in Figure 8.

We then studied the effect of increasing the time interval, Δt, between "data" points to 1 min (reference value = 0.5 min). The alternate "data" points from the reference case (Figs. 1 and 2) were used for this purpose. The results obtained showed an equally good fit of the viscosity data as that for the reference case. Figure 14 shows that the degree of ringing in a_1–d_1, with $\Delta t = 1$ min, is much less. The prediction capabilities and the final values of x_m, M_n, and M_w were found to be as good as for the reference case. The CPU time was 10 s. It is, thus, observed that larger values of Δt and narrower bounds on a_1–d_1 than used for the reference case are to be used for on-line control work. However, for experimental implementation, Δt has to be chosen keeping the criteria for sampling-period selection in mind.

We then explored the reasons for getting ringing in the values of the parameters. Isothermal (50°C) "data" on $\eta(t)$, without any fluctuations introduced, were taken. This is shown in Figure 15. The entire set of 66 points were curve-fitted to yield single values of the four parameters a_1–d_1 as shown by curves *A* in Figure 16. The same "data" were curve-fitted using 35 data points each, with four overlapping points (see Table III). Curves *B* in Figure 16 show sudden and significant changes in the value of at least one parameter, c_1. Cases *C* and *D* in Figure 16 show a significant amount of ringing as the number of curve-

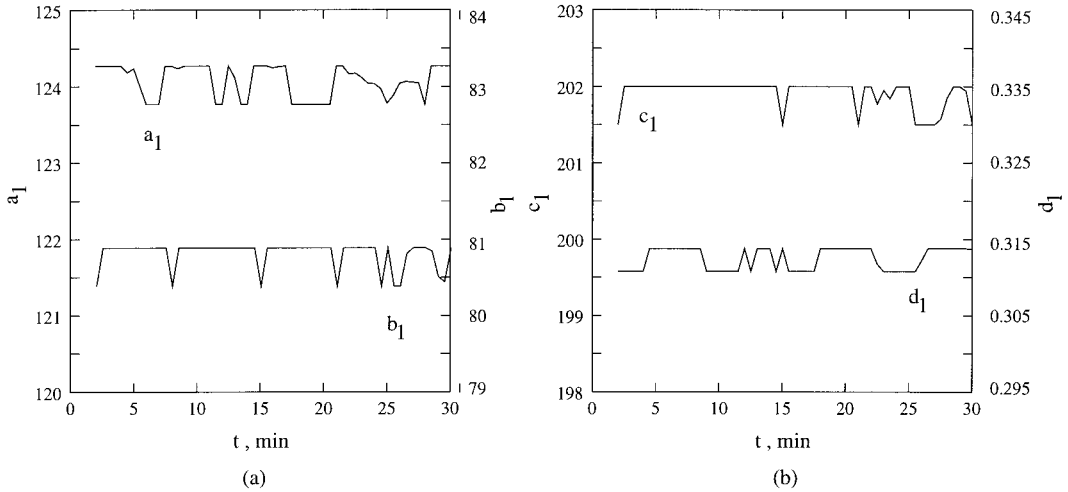

Figure 11 Variations of a_1–d_1 for the case when their bounds (Table II) are narrowed down by 50%.

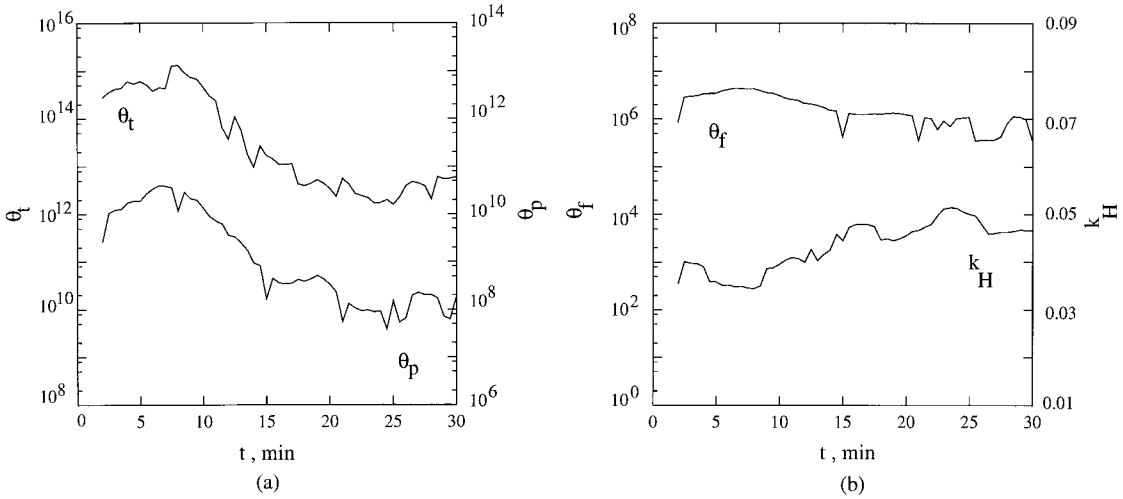

Figure 12 Variation of the parameters $\theta_t(T)$, $\theta_p(T)$, $\theta_f(T)$, and $k_H(T)$ corresponding to the curve-fit of Figure 11.

fitting horizons is increased. The fit of viscosity is equally good (as shown in Fig. 15 by the solid curve) in all the cases. It is, thus, clear that ringing is introduced by the use of only a few data points of viscosity, at a time, and that it is not caused by fluctuations in the data. The long-term predictions (for $N_1 = 5$), again, could be excellent or poor, because of the ringing in the values of the parameters.

Model Predictive Control

The estimated values of the kinetic parameters, θ_t, θ_p, θ_f, and k_H, at any time t, can be used to calculate the control action using an analytical model-predictive control scheme. The following optimization problem needs to be solved:

$$\text{Min} \sum_i A_1(x_{m,i,\text{mp}} - x_{m,i,\text{sp}})^2 + (\mu_{n,i,\text{mp}} - \mu_{n,i,\text{sp}})^2$$

$$\text{st: model equations and bounds on manipulated variables} \quad (8)$$

In eq. (8), the subscript mp stands for the model predicted and the subscript sp stands for set point or target values. Index, i, represents the (future) control horizon, and optimization is carried out

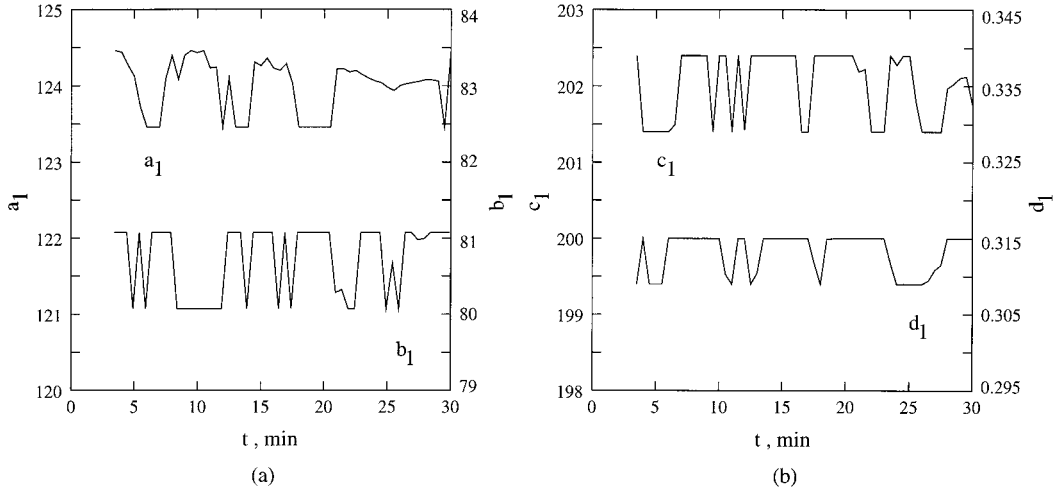

Figure 13 Variations of a_1–d_1 when N_1 is increased from 5 to 8.

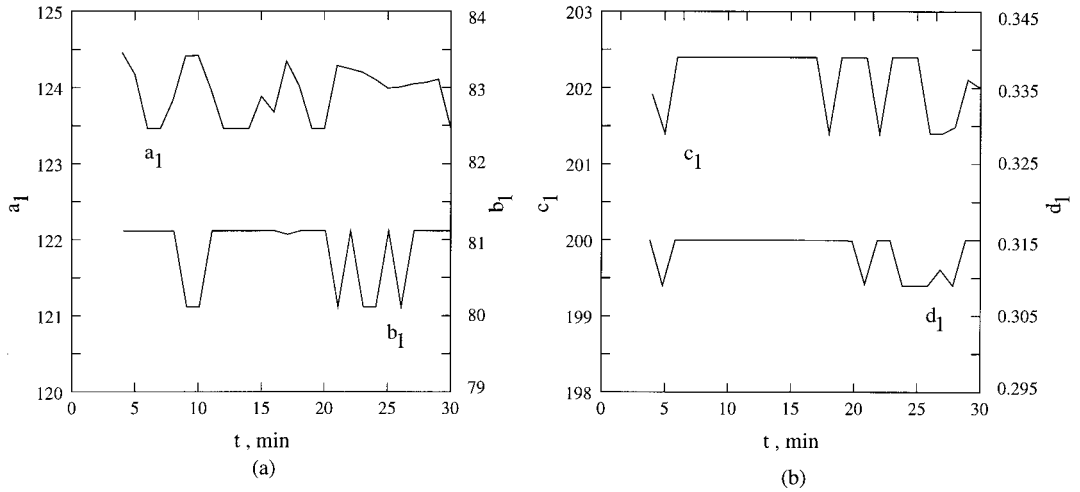

Figure 14 Variations of a_1–d_1 when Δt is increased from 0.5 to 1 min.

over the manipulated variable, which is the temperature of the reaction mass in the present case. A_1 and A_2, in eq. (8), are weightage factors. This technique allows prediction of the control action even when large disturbances enter the process or equipment failure occurs temporarily. If the monomer or initiator is added in between the polymerization process, this can be treated as a disturbance which can be automatically feed-forwarded and accounted for before it enters the process.

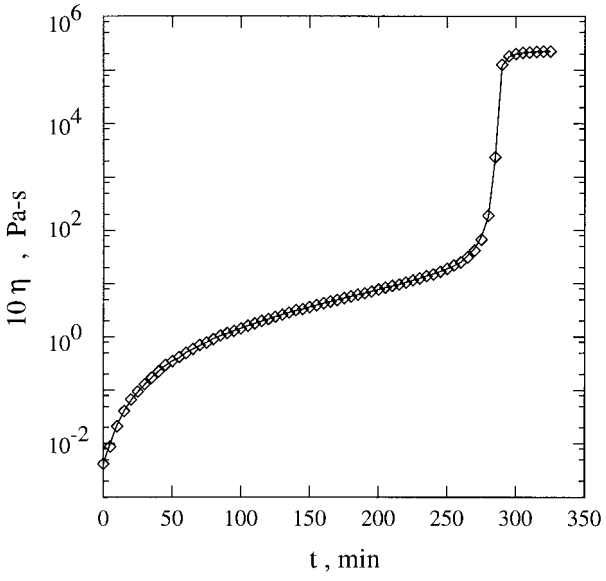

Figure 15 "Experimental" viscosity data (points) under isothermal (50°C) conditions with $[I]_0 = 15.48$ mol/m^3, in the absence of any randomization. Solid curve is the curve-fitted one, with $N_1 = 5$ and $N_3 = 1$.

On-line Optimization

The polymerization process is started using an off-line optimized temperature trajectory. However, usually, the trajectory can be followed only approximately because of experimental limitations (or disturbances enter the process, or material is added to or removed from the reactor, or equipment failure occurs temporarily). All these call for modifications of the remainder of the temperature trajectory. This can be easily done on-line using the present methodology. Experimental data up to time t_1 are used to calculate the model parameters which are used to estimate the state of the system. A fresh optimization is then carried out starting with the state as estimated above. This trajectory can then be followed until the end of the polymerization or until a new trajectory is found.

CONCLUSIONS

A model-based, inferential state-variable estimation technique has been described which uses a few of the most recent "data" points on temperature and the viscosity of the reaction mass (moving curve-fitting horizon) to predict x_m, μ_n, and μ_w. Short-term predictions in the moving prediction-horizon are found to be quite good, except when the curve-fitting horizon is very near to the gel-effect region and does not include any data point in this region. Multiple curve-fitting followed by periodic determination of the optimal temperature history in the remaining period of

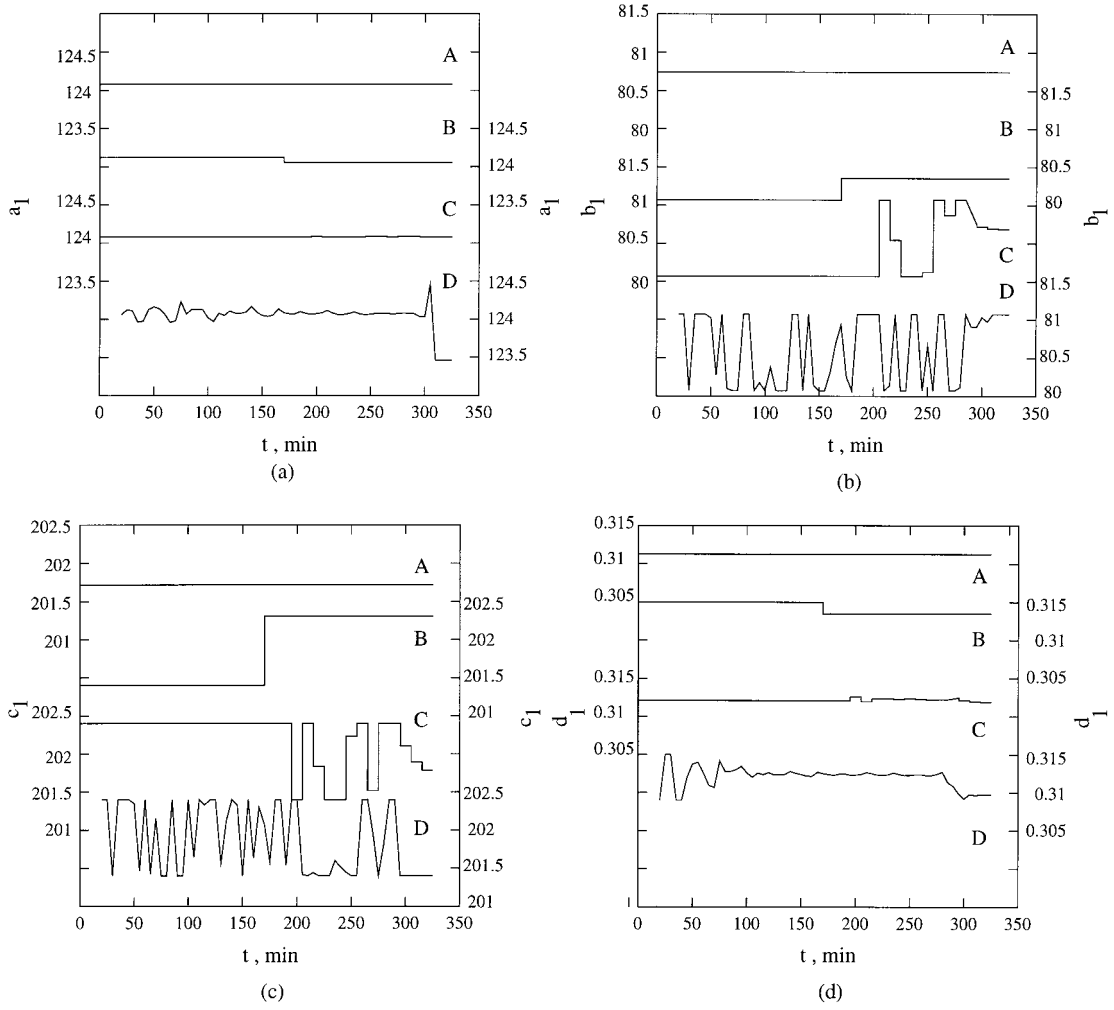

Figure 16 Variation of a_1–d_1 for the curve fitting of nonrandomized, isothermal (50°C) data shown in Figure 15. Values of N_1 and N_3 for the various cases are given in Table III. Scales for cases A and C are indicated on the left, while those for cases B and D are on the right-hand side.

polymerization could provide a satisfactory scheme for on-line optimizing control. It is possible to use experimental temperature and viscosity data in conjunction with the model equations to *uniquely* estimate the state of the system in terms of monomer conversion and weight-average molecular weight.

Table III Details of Parameters Used for Fitting Isothermal Viscosity Data of Figure 15 (Δt = 5 min)

Curve (Fig. 16)	N_1	N_3
A	66	—
B	35	31
C	40	2
D	05	1

NOMENCLATURE

a	parameter in the Mark–Houwink equation
a_1–a_3	parameters in correlation of θ_t
b	parameter in the Lyons–Tobolsky equation ($m^3\ kg^{-1}$)
b_1–b_3	parameters in correlation of θ_p
C_{polym}	concentration of polymer (kg m^{-3})
c_1–c_3	parameters in correlation of θ_f
D_n	dead polymer molecule having n repeating units

d_1, d_2	parameters in equation for k_H
E	objective function
E_d, E_p, E_t	activation energies for initiation, propagation, and termination in absence of gel or glass effects (kJ mol^{-1})
f	initiator efficiency
f_0	initiator efficiency in the limiting case of zero diffusional resistance
I	initiator (AIBN)
$[I]_0$	initial molar concentration of initiator (mol m^{-3})
K	parameter in the Mark–Houwink equation (m^3 kg^{-1})
k_H	Huggins' constant, dimensionless
k_d, k_f, k_i, k_p, k_s, k_{tc}, k_{td}	rate constants for the reactions in Table I at any time t (s^{-1} or m^3 mol^{-1} s^{-1})
k_t	$k_{tc} + k_{td}$
k_d^0, $k_{p,0}^0$, $k_{t,0}^0$	frequency factors for initiation, propagation, and termination in absence of the gel and glass effects (s^{-1} or m^3 mol^{-1} s^{-1})
$k_{t,0}$, $k_{p,0}$, $k_{i,0}$	k_t, k_p, and k_i in absence of gel and glass effects (m^3 mol^{-1} s^{-1})
M	moles of monomer (MMA) in liquid phase, mol
M_{jp}	molecular weight of polymer jumping unit (kg mol^{-1})
M_n	number-average molecular weight = $(MW_m)(\lambda_1 + \mu_1)/(\lambda_0 + \mu_0)$ (kg mol^{-1})
M_w	weight-average molecular weight = $(MW_m)(\lambda_2 + \mu_2)/(\lambda_1 + \mu_1)$ (kg mol^{-1})
(MW_I), (MW_m), (MW_s)	molecular weights of pure initiator, monomer, and solvent (kg mol^{-1})
N_1	number of points in the curve-fit horizon
N_2	number of points in the prediction horizon
N_3	number of data points to be deleted from the previous curve-fit horizon
P_n	growing polymer radical having n repeat units
R	primary radical; random number
R	universal gas constant (atm-m^3 mol^{-1} K^{-1})
R_{li}, R_{lm}, R_{ls}	rate of continuous addition of (liquid) initiator, monomer, and solvent to reactor (mol s^{-1})
R_{vm}, R_{vs}	rate of evaporation of monomer or solvent (mol s^{-1})
S	solvent
$S^\bullet$	solvent radical
T	temperature of reaction mixture at time t, K
t	time (min)
t_1	time at which state estimation is made (min)
V_1	volume of liquid at time t (m^3)
V_{fm}, V_{fp}, V_{fs}	fractional free volumes of monomer, polymer, and solvent in reaction mixture
$\hat{V}_I^*$, $\hat{V}_m^*$, $\hat{V}_p^*$, $\hat{V}_s^*$	specific critical hole free volumes of initiator, monomer, polymer, and solvent (m^3 kg^{-1})
$\mathbf{x}$	vector representing state variables
x_m	monomer conversion (molar) at time t

Greek Letters

γ	overlap factor
ζ_m, ζ_{m1}	net monomer added to the reactor
η	viscosity of the reaction mass (Pa-s)
$[\eta]$	intrinsic viscosity (m^3 kg^{-1})
η_{sol}	solvent (monomer) viscosity (Pa-s)
θ_f, θ_p, θ_t	adjustable parameters in the model for cage, glass, and gel effects, respectively (m^3 mol^{-1}, s, s)
λ_k	kth ($k = 0, 1, 2, \ldots$) moment of live (P_n) polymer radicals $\equiv \Sigma_{n=1}^{\infty} n^k P_n$ (mol)
μ_k	kth ($k = 0, 1, 2, \ldots$) moment of dead (D_n) polymer chains $\equiv \Sigma_{n=1}^{\infty} n^k D_n$ (mol)
μ_n	number-average chain length at time t $\equiv (\lambda_1 + \mu_1)/(\lambda_0 + \mu_0)$
μ_w	weight-average chain length at time t $\equiv (\lambda_2 + \mu_2)/(\lambda_1 + \mu_1)$
ξ_{13}, ξ_{23}, ξ_{I3}	ratio of the molar volume of the monomer, solvent, and initiator jumping units to the critical molar volume of the polymer, respectively
ρ_m, ρ_p, ρ_s	density of pure (liquid) monomer, polymer or solvent at temperature T (at time t) (kg m^{-3})

ϕ_m, ϕ_p, ϕ_s volume fractions of monomer, polymer, or solvent in liquid at time t
ψ, ψ_{ref} defined in eqs. (A.20) and (A.21) in Appendix A

Subscripts/Superscripts

exp	experimental value
mp	model-predicted value
Min	minimize
0	initial value
sm	smooth
sp	set point value
th	theoretical value

APPENDIX A: MODEL EQUATIONS FOR MMA POLYMERIZATION IN SEMIBATCH REACTORS[12] (BULK AND SOLUTION POLYMERIZATION*)

$$\frac{dI}{dt} = -k_d I + R_{li}(t) \tag{A.1}$$

$$\frac{dM}{dt} = -(k_p + k_f)\frac{\lambda_0 M}{V_1} - k_i \frac{RM}{V_1} - k_s S \frac{\lambda_0}{V_1} + R_{lm}(t) - R_{vm}(t) \tag{A.2}$$

$$\frac{dR}{dt} = 2fk_d I - k_i \frac{RM}{V_1} \tag{A.3}$$

$$\frac{dS}{dt} = R_{ls}(t) - R_{vs}(t) \tag{A.4}$$

$$\frac{d\lambda_0}{dt} = k_i \frac{RM}{V_1} - k_t \frac{\lambda_0^2}{V_1} \tag{A.5}$$

$$\frac{d\lambda_1}{dt} = k_i \frac{RM}{V_1} + k_p M \frac{\lambda_0}{V_1} - k_t \frac{\lambda_0 \lambda_1}{V_1} + (k_s S + k_f M)\frac{(\lambda_0 - \lambda_1)}{V_1} \tag{A.6}$$

$$\frac{d\lambda_2}{dt} = k_i \frac{RM}{V_1} + k_p M \frac{\lambda_0 + 2\lambda_1}{V_1} - k_t \frac{\lambda_0 \lambda_2}{V_1} + (k_s S + k_f M)\frac{(\lambda_0 - \lambda_2)}{V_1} \tag{A.7}$$

$$\frac{d\mu_0}{dt} = (k_s S + k_f M)\frac{\lambda_0}{V_1} + \left(k_{td} + \frac{1}{2}k_{tc}\right)\frac{\lambda_0^2}{V_1} \tag{A.8}$$

$$\frac{d\mu_1}{dt} = (k_s S + k_f M)\frac{\lambda_1}{V_1} + k_t \frac{\lambda_0 \lambda_1}{V_1} \tag{A.9}$$

$$\frac{d\mu_2}{dt} = (k_s S + k_f M)\frac{\lambda_2}{V_1} + k_t \frac{\lambda_0 \lambda_2}{V_1} + k_{tc}\frac{\lambda_1^2}{V_1} \tag{A.10}$$

$$\frac{d\xi_m}{dt} = R_{lm}(t) - R_{vm}(t) \tag{A.11}$$

$$\frac{d\xi_{m_1}}{dt} = R_{lm}(t) \tag{A.12}$$

$$V_1 = \frac{S(MW_s)}{\rho_s} + \frac{M(MW_m)}{\rho_m} + \frac{(\xi_m - M)(MW_m)}{\rho_p} \tag{A.13}$$

$$\phi_m = \frac{M(MW_m)/\rho_m}{\frac{M(MW_m)}{\rho_m} + \frac{S(MW_s)}{\rho_s} + \frac{(\xi_m - M)(MW_m)}{\rho_p}} \tag{A.14}$$

$$\phi_s = \frac{S(MW_s)/\rho_s}{\frac{M(MW_m)}{\rho_m} + \frac{S(MW_s)}{\rho_s} + \frac{(\xi_m - M)(MW_m)}{\rho_p}} \tag{A.15}$$

$$\phi_p = 1 - \phi_m - \phi_s \tag{A.16}$$

$$\frac{1}{f} = \frac{1}{f_0}\left[1 + \theta_f(T)\frac{M}{V_1}\frac{1}{\exp[\xi_{I3}\{-\psi + \psi_{ref}\}]}\right] \tag{A.17}$$

$$\frac{1}{k_t} = \frac{1}{k_{t,0}} + \theta_t(T)\mu_n^2 \frac{\lambda_0}{V_1}\frac{1}{\exp[-\psi + \psi_{ref}]} \tag{A.18}$$

$$\frac{1}{k_p} = \frac{1}{k_{p,0}} + \theta_p(T)\frac{\lambda_0}{V_1}\frac{1}{\exp[\xi_{13}\{-\psi + \psi_{ref}\}]} \tag{A.19}$$

$$\psi = \frac{\gamma\left\{\frac{\rho_m \phi_m \hat{V}_m^*}{\xi_{13}} + \frac{\rho_s \phi_s \hat{V}_s^*}{\xi_{23}} + \rho_p \phi_p \hat{V}_p^*\right\}}{\rho_m \phi_m \hat{V}_m^* V_{fm} + \rho_s \phi_s \hat{V}_s^* V_{fs} + \rho_p \phi_p \hat{V}_p^* V_{fp}} \tag{A.20}$$

* No inert solvent (benzene) used in this work. Variables not defined in the Nomenclature are defined in Refs. 7 and 12.

$$\psi_{\text{ref}} = \frac{\gamma}{V_{\text{fp}}} \tag{A.21}$$

$$\xi_{13} = \frac{\hat{V}_m^*(\text{MW}_m)}{\hat{V}_p^* M_{\text{jp}}} \tag{A.22}$$

$$\xi_{23} = \frac{\hat{V}_s^*(\text{MW}_s)}{\hat{V}_p^* M_{\text{jp}}} \tag{A.23}$$

$$\xi_{I3} = \frac{\hat{V}_I^*(\text{MW}_I)}{\hat{V}_p^* M_{\text{jp}}} \tag{A.24}$$

$$k_d = k_d^0 \exp(-E_d/RT) \tag{A.25}$$

$$k_{p,0} = k_{p,0}^0 \exp(-E_p/RT) \tag{A.26}$$

$$k_{t,0} = k_{\text{td},0} = k_{\text{td},0}^0 \exp(-E_{\text{td}}/RT) \tag{A.27}$$

$$\eta = \eta_{\text{sol}} \left[1 + C_{\text{polym}}[\eta] \exp\left(\frac{k_H[\eta] C_{\text{polym}}}{1 - bC_{\text{polym}}} \right) + C_{\text{polym}}^2[\eta]^2 \exp\left(\frac{2k_H[\eta] C_{\text{polym}}}{1 - bC_{\text{polym}}} \right) \right] \tag{A.28}$$

$$C_{\text{polym}} = \rho_p \phi_p \tag{A.29}$$

$$[\eta] = K M_w^a \tag{A.30}$$

APPENDIX B: PARAMETERS USED FOR BULK POLYMERIZATION OF MMA WITH AIBN[12]

$\rho_m = 966.5 - 1.1(T - 273.1)$ kg/m^3

$\rho_p = 1200$ kg/m^3

$f_0 = 0.58$

$k_d^0 = 1.053 \times 10^{15}$ s^{-1}

$k_{p,0}^0 = 4.917 \times 10^2$ m^3/mol-s

$k_{\text{td},0}^0 = 9.8 \times 10^4$ m^3/mol-s

$k_{\text{tc}} = 0.0$

$k_f = 0.0$

$k_i = k_p$

$k_s = 0.0$

$E_d = 128.45$ kJ/mol

$E_p = 18.22$ kJ/mol

$E_{\text{td}} = 2.937$ kJ/mol

$(\text{MW}_m) = 0.10013$ kg/mol

$(\text{MW}_I) = 0.06800$ kg/mol

Parameters for the Cage, Gel and Glass Effects

$\hat{V}_I^* = 9.13 \times 10^{-4}$ m^3/kg

$\hat{V}_m^* = 8.22 \times 10^{-4}$m^3/kg

$\hat{V}_p^* = 7.70 \times 10^{-4}$ m^3/kg

$M_{\text{jp}} = 0.18781$ kg/mol

$\gamma = 1$

$V_{\text{fm}} = 0.149 + 2.9 \times 10^{-4}[T(K) - 273.1]$

$V_{\text{fp}} = 0.0194 + 1.3 \times 10^{-4}[T(K) - 273.1 - 105]$; for $T < (105 + 273.1)K$

Mark–Houwink Constants for Intrinsic Viscosity [See Eq. (29), Appendix A]

$K = 6.75 \times 10^{-6}$ m^3/kg

$a = 0.72$

K and a assumed to be (almost) independent of T.

Parameters for the Adapted Lyons–Tobolsky Equation [Eq. (28), Appendix A]

$k_H = -d_1 + d_2 T$

$d_1 = 0.3118$; $d_2 = 9.93 \times 10^{-4}\ K^{-1}$ (this work)

$b = -3.5 \times 10^{-3}$ m^3/kg (assumed independent of T)

$\eta_{\text{sol}} = \exp(-0.099 + 496/T)/T^{1.5939}$ Pa-s (Ref. 5)

Correlations Used for Curve-Fitting

$$\log_{10}[\theta_t(T), \text{s}] = a_1 - a_2(1/T) + a_3(1/T^2)$$

$$\log_{10}[\theta_p(T), \text{s}] = b_1 - b_2(1/T) + b_3(1/T^2)$$

$$\log_{10}[10^3 \theta_f(T), \text{m}^3\ \text{mol}^{-1}] = c_1 - c_2(1/T) + c_3(1/T^2)$$

$a_1 = 1.2408 \times 10^2$; $a_2 = 1.0314 \times 10^5$; $a_3 = 2.2735 \times 10^7$

$b_1 = 8.0593 \times 10^1$; $b_2 = 7.5 \times 10^4$; $b_3 = 1.765 \times 10^7$

$c_1 = 2.016 \times 10^2$; $c_2 = 1.455 \times 10^5$;

$c_3 = 2.70 \times 10^7$ (this work)

REFERENCES

1. R. G. W. Norrish and R. R. Smith, *Nature,* **150,** 336 (1942).
2. E. Trommsdorff, H. Kohle, and P. Lagally, *Makromol. Chem.,* **1,** 169 (1947).
3. W. Y. Chiu, G. N. Carratt, and D. S. Soong, *Macromolecules,* **16,** 348 (1983).
4. D. Achilias and C. Kiparissides, *J. Appl. Polym. Sci.,* **35,** 1303 (1988).
5. D. S. Achilias and C. Kiparissides, *Macromolecules,* **25,** 3739 (1992).
6. J. S. Vrentas and J. L. Duda, *AIChE J.,* **25,** 1 (1979).
7. A. B. Ray, D. N. Saraf, and S. K. Gupta, *Polym. Eng. Sci.,* **35,** 1290 (1995).
8. S. T. Balke and A. E. Hamielec, *J. Appl. Polym. Sci.,* **17,** 905 (1973).
9. G. V. Schultz and G. Harborth, *Makromol. Chem.,* **1,** 106 (1947).
10. T. Srinivas, S. Sivakumar, S. K. Gupta, and D. N. Saraf, *Polym. Eng. Sci.,* **36,** 311 (1996).
11. V. Dua, D. N. Saraf, and S. K. Gupta, *Polym. Eng. Sci.,* **59,** 749 (1996).
12. V. Seth and S. K. Gupta, *J. Polym. Eng.,* **15,** 283 (1995).
13. M. Soroush and C. Kravaris, *AIChE J.,* **38,** 1429 (1992).
14. M. F. Ellis, T. W. Taylor, and K. F. Jensen, *AIChE J.,* **40,** 445 (1994).
15. T. J. Crowley and K. Choi, *J. Process Control,* **6,** 119 (1996).
16. S. S. S. Chakravarthy, D. N. Saraf, and S. K. Gupta, *J. Appl. Polym. Sci.,* **63,** 529 (1997).
17. M. Embirucu, E. L. Lima, and J. C. Pinto, *Polym. Eng. Sci.,* **36,** 433 (1996).
18. S. K. Gupta, *Numerical Methods for Engineers,* New Age International/Wiley Eastern, New Delhi, 1995.
19. H. U. Moritz, *Chem. Eng. Technol.,* **12,** 71 (1989).
20. P. F. Lyons and A. V. Tobolsky, *Polym. Eng. Sci.,* **10,** 1 (1970).
21. R. B. Mankar, P. Ghosh, D. N. Saraf, and S. K. Gupta, to appear.
22. P. E. Gill, W. Murray, and M. H. Wright, *Practical Optimization,* Academic Press, New York, 1981.
23. R. Sareen and S. K. Gupta, *J. Appl. Polym. Sci.,* **58,** 2357 (1995).